

Supporting Information

Propagating Precipitation Waves in Disordered Media

Takahiko Ban,^{*,†} Masaru Kaji,^{‡,§} Yuichiro Nagatsu^{||} and Hideaki Tokuyama^{||}

[†]*Division of Chemical Engineering, Department of Materials Engineering Science, Graduate School of Engineering Science, Osaka University, Machikaneyamacho 1-3, Toyonaka City, Osaka 560-8531, Japan*

[‡]*Graduate School of Decision Science and Technology, Tokyo Institute of Technology, 2-12-1 Ookayama, Meguro-ku, Tokyo 152-8552, Japan*

[§]Japan Society for the Promotion of Science, 8 Ichibancho, Kojimachi, Chiyoda-ku, Tokyo, 102-8472, Japan

^{||}Department of Chemical Engineering, Tokyo University of Agriculture and Technology, 2-24-16 Naka-cho, Koganei, Tokyo 184-8588, Japan

Corresponding author: Takahiko Ban

Tel:+81-6-6850-6625, Fax: +81-6-6850-6625

E-mail: ban@cheng.es.osaka-u.ac.jp

- Movie 1. Single ring-like wave of precipitation reaction for $C_{Al} = 0.24 \text{ M}$ and $T_q = 25 \text{ }^\circ\text{C}$. The movie is at 150 x speed.
- Movie 2. Target-like waves of precipitation reaction for $C_{Al} = 0.28 \text{ M}$ and $T_q = 25 \text{ }^\circ\text{C}$. The movie is at 150 x speed.
- Movie 3. Spiral-like waves of precipitation reaction for $C_{Al} = 0.30 \text{ M}$ and $T_q = 25 \text{ }^\circ\text{C}$. Transition of target-like waves to spiral-like waves owing asymmetric collision of both ends of precipitation wave is displayed in the lower corner of the screen. The movie is at 150 x speed.
- Movie 4. Collapsing pattern of precipitation reaction for $C_{Al} = 0.32 \text{ M}$ and $T_q = 25 \text{ }^\circ\text{C}$. The movie is at 150 x speed.
- Movie 5. Turbulence pattern of precipitation reaction for $C_{Al} = 0.40 \text{ M}$ and $T_q = 25 \text{ }^\circ\text{C}$. The movie is at 150 x speed.
- Movie 6. Two transition processes of precipitation reaction for $C_{Al} = 0.29 \text{ M}$ and $T_q = 25 \text{ }^\circ\text{C}$. One is the transition of target-like waves to spiral-like waves because of asymmetric collision, displayed in the upper right corner of the screen. The other is the transition of target-like waves to a single expanding ring-like wave owing to the head-on collision which is displayed in the right of the screen. The movie is at 150 x speed.

Characterization of agar gel

Diffusion coefficient of the outer electrolyte in the gel

The gel membrane was prepared and a permeability test was carried out. Hot agar solution without AlCl_3 was poured into the central hole of an acrylic resin mold (support) and covered with two glass plates. A gel membrane specimen with a diameter of 10 mm and thickness of 3.1 mm was prepared by quenching at different temperatures (10–40 °C). The glass plates were removed and the resultant gel membrane was washed with water. The support with the gel membrane was placed between two cells. An aqueous solution (31 cm^3) containing 10 mol/m^3 NaOH was poured into the upstream cell and water (30 cm^3) was poured into the downstream cell. The solutions were stirred at 25 °C. The concentration of NaOH in the downstream cell was measured by monitoring the electrical conductivity of the solution using an electric conductivity meter (HORIBA Ltd., F-74SP). The concentration of NaOH, C [mol/m^3], in the downstream cell increased linearly with time, t , after an initial time lag. The diffusion coefficient, D [m^2/s], of NaOH through the gel membrane was determined using the following equation based on the Fickian diffusion equation [2]:

$$D = [Vd/(AC_0)](dC/dt) \quad (\text{S1})$$

where V is the volume of solution in the downstream cell, d is the thickness of the membrane, A is the cross-sectional area of the membrane, and C_0 is the initial concentration of NaOH in the upstream cell. The relationship between the values of D and the quenching temperature is shown in Figure S1.

[1] A. Takahashi, and S. Sakohara, *J Appl Polym Sci* **124**, 1208(2012).

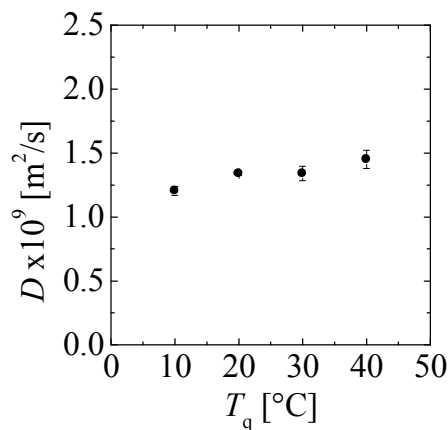


Figure S1 Relationship between the diffusion coefficient, D of NaOH as the outer electrolyte through the agar gel membrane and quenching temperature.

Mechanical properties of the agar gel

A disc-shaped gel specimen with a diameter of 5 mm and thickness of 2 mm was prepared and a compression test was carried out. Hot agar solution without AlCl_3 was poured into the mold and quenched at different temperatures (10–40 °C). The shear modulus, μ , and compressive strength, F_c , of the gel were measured at 20°C by the compression technique [3,4] using a rheometer (TA Instruments, AR-G2). The μ value was determined from the linear relationship between the stress ΔP and the compressive deformation length ratio, $\Delta l/l_0$, using the relationship $\Delta P = 3\mu (\Delta l/l_0)$, where $\Delta l/l_0 = (l - l_0)/l_0$ and l_0 and l are the lengths of the gel before and after compression, respectively. The value of F_c was determined by dividing the stress when the gel fractured by the initial cross-sectional area of the gel.

[2] T. Tanaka, L. O. Hocker, and G. B. Benedek, J. Chem. Phys. **59**, 5151 (1973) .

[3] R. Sato, R. Noma, and H. Tokuyama, Eur Polym J **66**, 91 (2015).

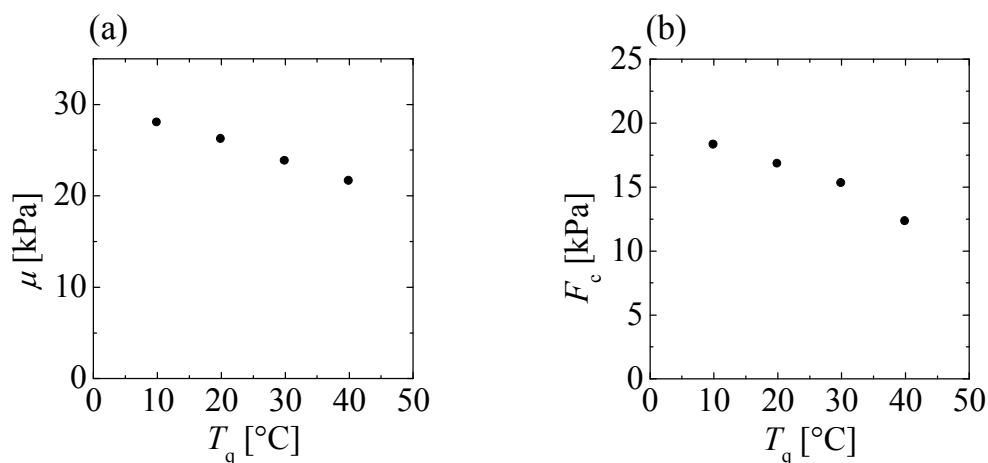


Figure S2 (a) Relationship between the shear modulus μ and quenching temperature. (b) Relationship between the compressive strength F_c and quenching temperature.

Pattern formation of target and spiral-like waves

Figure S3 shows the formation process of the target-like waves and the transition of these target-like waves into spiral-like waves (see Movie 3). The target-like waves from the precipitation reaction originate due to the collision of two counterrotating arms of the precipitation waves. The two ends of the precipitation waves extend right and left, with the left and right arms curling clockwise and counter-clockwise, respectively (Figs. S3a and S3b). The two curled arms collide between the outward interface of the wave fronts (Fig. S3c), which leads to separation of the arms into two parts: a tip that breaks away from the point of collision, and a remaining part that is similar to a distorted ring wave (Fig. S3d). The tip that breaks off remains within the distorted ring wave and extends right and left again to grow into a new curled precipitation wave. The two ends of this curled tip precipitation wave again collide with each other. On the other hand, the distorted ring-like part extends outward and changes into a circular ring-like wave. This series of events is repeated, leading to the formation of the target-like waves. If a head-on collision of the two ends of the precipitation wave were to occur, no separation of the arms into two parts would occur; the target-like waves would no longer be generated and instead a single expanding ring-like wave would form (see Movie 6). Thus, the experimental results indicate that, in contrast to the case for the BZ reaction, the gel in the precipitation system here does not behave like an oscillatory medium.

The spiral-like waves are generated from the collision of the asymmetric curled arms (see Movie S4). After the formation of several target-like waves due to repeated symmetric collisions, the separated tip of the precipitation wave transforms into asymmetric curled arms with different radii of curvature (Fig. S3e). The end of the precipitation wave with the larger radius of curvature collides with the outward interface of the precipitation wave with the smaller radius of curvature (Fig. S3f). The two ends of the resulting separated fraction of the precipitation wave with the smaller radius of curvature extends asymmetrically and transforms into a clockwise spiral-like wave within the circular target waves (Figs. S3g and S3h). In this way, the spiral-like waves are generated from the asymmetric growth of the target-like waves.

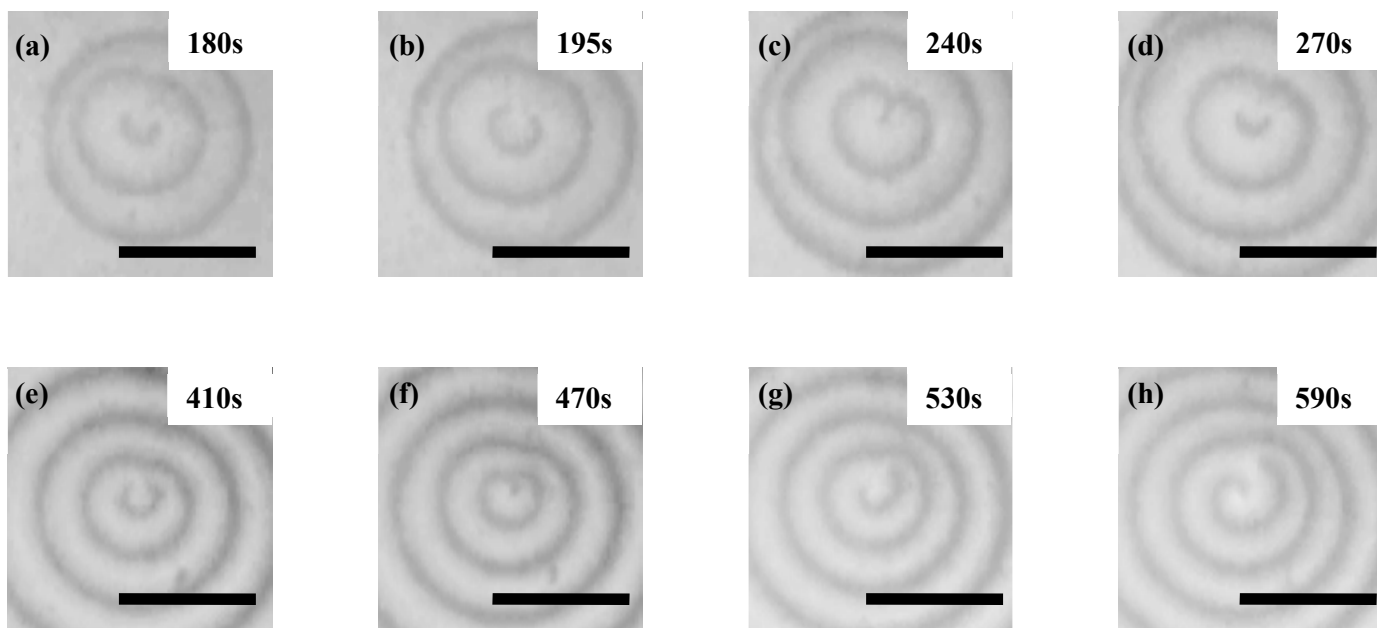






















Figure S3 Evolution of target-like waves (a – d) and spiral waves (e – h) for $C_{AI} = 0.29$ M. The numbers in the figure represent the elapsed time after the outer electrolyte diffuses into the gel. Scale bars are 2 mm.

Phase diagram of precipitation pattern in the precipitation reaction temperature and Al concentration space

We investigated the effect of the precipitation reaction temperature on the pattern formation of precipitation waves. Agar gel containing different concentrations of the outer electrolyte was prepared in a Petri dish at the constant quenching temperature, $T_q = 25^\circ\text{C}$. The petri dish was introduced in a thermostatic bath. 20 mL of a 2.5 M NaOH solution was poured into the formed gel and the reaction was observed at different precipitation reaction temperatures. Table S1 shows the relationship between the precipitation reaction temperature and pattern formation in 60 min after the start of the precipitation reaction. The precipitation reaction temperature has no effect on the pattern formation of precipitation waves.

Table S1 Relationship between the precipitation reaction temperature and pattern formation in 60 min after the start of the precipitation reaction at $T_q = 25^\circ\text{C}$.

AlCl_3 [mol/l]	Reaction temperature [$^\circ\text{C}$]				
	25	30	35	40	45
0.28					
0.30					
0.35					
0.40					

Dynamics of single ring-like wave

Figure S4a shows the change in the radius, r , of the single ring-like pattern for different T_q values at $C_{Al} = 0.25$ M. The dynamics are in keeping with the diffusion process, with $r(t) = 2\sqrt{D_r t}$ (D_r : effective diffusion coefficient; t : time).

We evaluated the dynamics of the single ring-like pattern at $C_{Al} = 0.25$ M. Figure S4a shows that the dynamics are in keeping with the diffusion process, with $r(t) = 2\sqrt{D_r t}$. We calculated the effective diffusion coefficient of the single ring-like pattern from this expression. The effective diffusion coefficient increases with T_q even at the constant precipitation reaction temperature. Although the macroscopic properties increase by only 20–30% with an increase in T_q from 10 to 40 °C, the effective diffusion coefficient increases by a factor of three. Thus, the increase in effective diffusion coefficient reflects the change in the gel structure. The increase in T_q leads to an increase in the correlation length of the composition fluctuations, which changes the permeability of the gel and leads to an improvement in the mobility of the precipitation reaction waves.

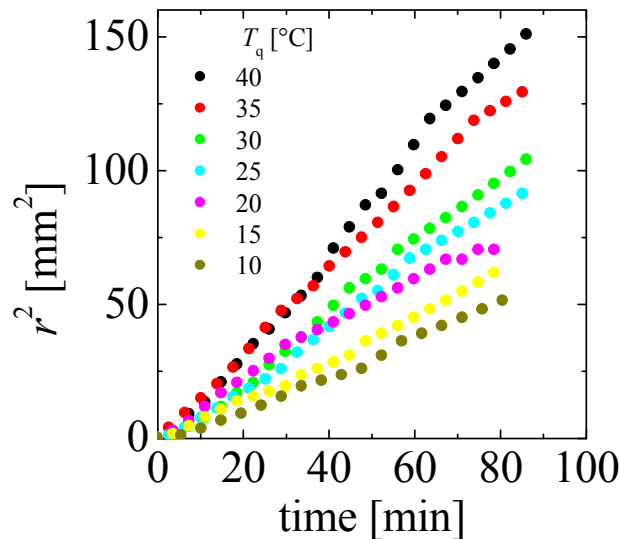


Figure S4. Radius of single ring-like wave at different quenching temperatures for $C_{Al} = 0.25$ M. Vertical axis represents the square of the radius.

Dynamics of target-like waves

Figure S5 shows the change in radius of the target-like waves at $C_{AI} = 0.28 M$. Its dynamics deviates from those corresponding to the diffusion process as T_q is increased, with anomalous diffusion occurring at $r \sim t^\alpha$ ($\alpha > 0.5$). For $\alpha > 0.5$, the dynamics correspond to a phenomenon called superdiffusion. The exponential α for this system increases from 0.5 to approximately 0.75 with an increase in T_q .

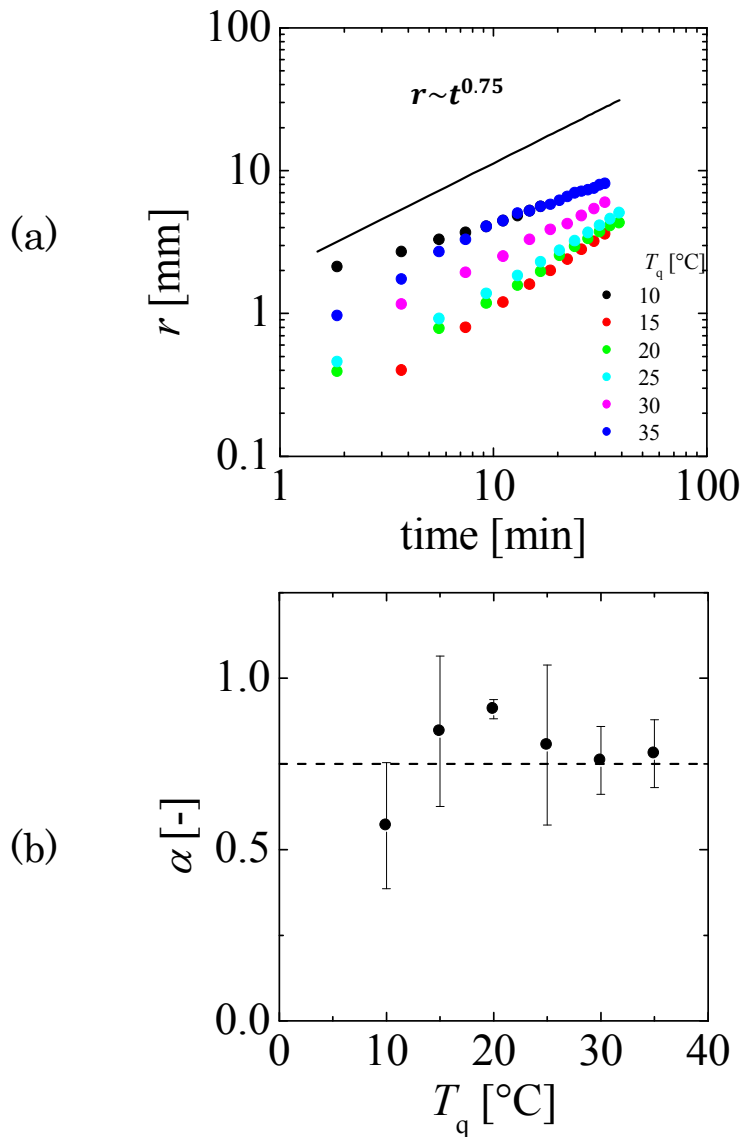


Figure S5 (a) Radius of target-like waves at different T_q values for $C_{AI} = 0.25 M$. Data for radius at $T_q = 40$ °C were removed because the pattern consisted of spiral-like waves. (b) Relation between the exponent α and T_q .

Dispersion relationship of target -like waves

We investigated the dispersion relationship between the angular frequency, ω ($= 2\pi/T$) and the wavenumber, k ($= 2\pi/\lambda$) for the target-like waves at $C_{Al} = 0.28$ M. The period, T , is defined as the duration of one cycle of the target-like pattern due to the collision of two counterrotating arms of a precipitation wave. The wavelength, λ , is measured between two adjacent target-like waves. Since a simple polynomial form ($\omega = a_0 + a_1k + a_2k^2 + a_3k^3 \dots$) cannot be used, we propose the following expression to evaluate the dispersion relationship:

$$\omega = \frac{D_{eff}k^2}{1 - \frac{k^2}{k_0^2}} \quad (S2)$$

with D_{eff} and k_0 the fitting parameters having dimensions of the diffusion coefficient and the wavenumber, respectively. Rearranging this equation yields:

$$\frac{1}{\omega} = \frac{1}{D_{eff}k^2} - \frac{1}{D_{eff}k_0^2} \quad (S3)$$

Plotting $1/\omega$ versus $1/k^2$ gives a straight line, whose gradient and intercept can be used to determine D_{eff} and k_0 . Figure S6 shows the plot of $1/\omega$ versus $1/k^2$. We obtained a linear relationship at each T_q allowing the calculation of D_{eff} and k_0 from Eq. (S3). The precipitation waves obeyed the specific dispersion relationship. While the physical meaning of the dispersion relationship remains unknown, the two fitting parameters showed a simple dependency on T_q . Thus, the empirical equation may be related to the geometrical disorder arising in the reaction matrix.

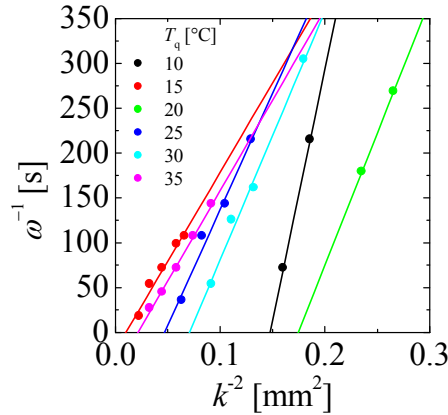
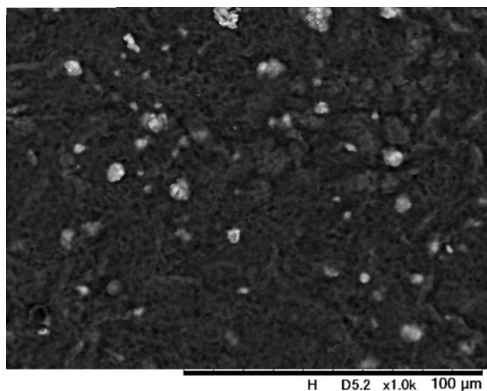


Figure S6. Dispersion relationship between angular frequency, ω , and wavenumber, k , for $C_{Al} = 0.28$ M for target-like waves. Data were obtained based on the plot of $1/\omega$ versus $1/k^2$. The gradient and intercept of a straight line were used to determine D_{eff} and k_0 from Eq. (3).

SEM observation

The gel specimens, where precipitation waves form, was removed in 60 min after the pour of 2.5 M NaOH solution into the gel. The sample gel specimens were prepared by freeze-drying the swollen gels and then coating them with gold. The internal structure of the gels was observed by scanning electron microscopy (Hitachi High-Technologies Co., Miniscope TM3030).

(a)



(b)

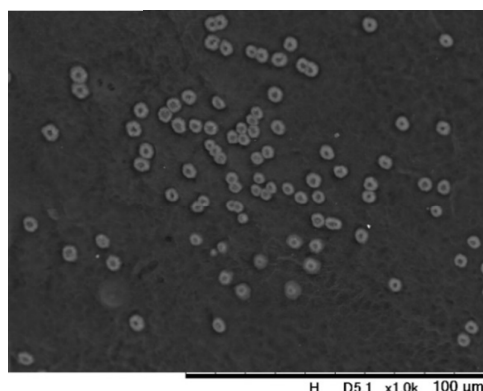


Figure S7. SEM image of the agar gel prepared as for (a) $C_{Al} = 0.25$ M and (b) $C_{Al} = 0.30$ M.